The first term of Stalder and Zurick's equation is

$$\frac{(1+2s^2)}{\sqrt{\pi}s^3}\exp\ (-s^2)$$

At $s=0.8$, Walsh's $C_D$ values are almost 10% higher than those calculated using Stalder and Zurick's equation for diffuse reflection. Thus, the set of 84 constants presented by Walsh for $0.1<M<2$ need to be revised to remove this error.

It is also of interest to consider Mach numbers greater than 1.75 and less than 0.1. Since both Walsh and this author use a Martino-type expression at $M>1.75$, both techniques should be capable of yielding the same degree of accuracy in this range. This is not true, however, at $M<0.1$. In Walsh's original presentation,[12] rarefaction effects are ignored at $M<0.1$; this leads to very large errors in $C_D$ values. In his comment, Walsh attempts to correct this problem by proposing his Eq. (5). Inspection of the form of Eq. (5), however, shows that it must fail at low Reynolds number. Consider, for example, $C_D$ at $M=Re=10^{-3}$. The continuum value of $C_D$ is $2.4\times10^4$ and the free molecular value is $5\times10^3$. The term $(M-M_{max})/(0.1-M_{max})$ in Walsh's Eq. (5), however, is $\sim10^{-2}$. Thus, at low $Re$, $C_D\cong C_{D2}$; this is equivalent to ignoring rarefaction effects and can lead to errors in $C_D$ as large as several orders of magnitude.

It is concluded that Walsh's correlation gives improved accuracy in a narrow range of Mach number and Reynolds number. Walsh's correlation is shown to fail at Mach numbers and Reynolds numbers less than 0.1. Finally, an error in Walsh's values for molecular flow $C_D$ requires a revision in his empirical parameters.

## References


[1]Walsh, M. J., "Drag Coefficient Equations for Small Particles in High Speed Flows," *AIAA Journal*, Vol. 13, Nov. 1975, pp. 1526-1528.

[2]Walsh, M. J., "Influence of Particle Drag Coefficient on Particle Motion in High-Speed Flow with Typical Laser Velocimetry Applications," NASA TND-8120, Feb. 1976.

[3]Henderson, C. B., "Drag Coefficients of Spheres in Continuum and Rarefied Flows," *AIAA Journal*, Vol. 14, June 1976, pp. 707-708.

[4]Bailey, A. B., and Hiatt, J., "Free-Flight Measurements of Sphere Drag at Subsonic, Transonic, and Supersonic Speeds for Continuum, Transition, and Near-Molecular Flows," Arnold Engineering Development Center, Arnold Air Force Station, Tenn., TR-70-291, March 1971.

[5]Schaaf, S. A., and Chambre, P. L., "Flow of Rarefied Gases," Emmons, H. W., Ed., *Fundamentals of Gas Dynamics*, Vol. III, High Speed Aerodynamics and Jet Propulsion," Princeton University Press, Princeton, N.J., 1958, p. 704.

[6]Stalder, J. and Zurick, V., "Theoretical Characteristics of Bodies in a Free Molecule Flow Field," NASA TN 2423, 1951.


# Comment on "Experimental Investigation of the Boundary Layer on a Rotating Cylinder"


E.E. Covert*
*MIT, Cambridge, Mass.*


IN Ref. 1, Morton et al. presented an excellent review of their experimental data on the characteristics of boundary layers on rotating cylinders. These data were reduced to the form of the distribution of displacement thickness and compared with predictions based upon J.C. Martin's theory (Ref. 2, herein; note this is Ref. 7 of Morton et al.). The purpose of these remarks is to clarify application of Martin's theoretical results to Morton's expansion of the three-dimensional boundary layer equation, including second order. The expansion contains a primary implicit assumption that the boundary layer thickness $\delta$ is much less than the radius of the cylinder $r$. For the data presented in Ref. 1, $0.07\leq\delta/r\leq0.17$, so the implicit assumption is satisfied, more or less.


Received Feb. 1, 1976.
Index category: Boundary-Layer Stability and Transition.


*Professor of Aeronautics and Astronautics. Fellow AIAA.

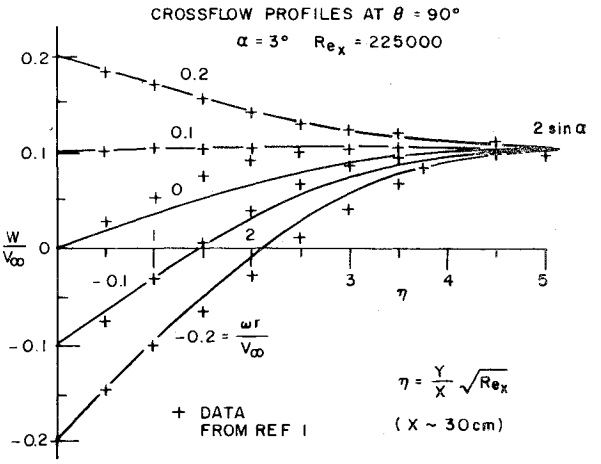


**Fig. 1 Azimuthal velocity distribution for several spin rates.**

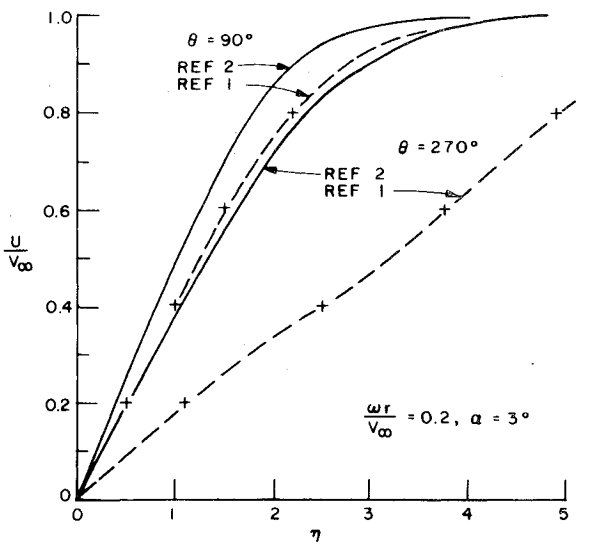


**Fig. 2 Longitudinal velocity distribution through the boundary layer.**

As Martin points out, his expansion scheme involves a number of dimensionless groups. The group of importance to this discussion is the product of the angle of attack $\alpha$ and the axial position measured in radii $(\alpha x/r)$. Its size is shown for several lengthwise positions, along the cylinder; for $x(cm)=$ 20, 30, 40, and 50; $(\alpha x/r)=0.37$, 0.55, 0.73, and 0.92; respectively. Assuming the series expansion in $(\alpha x/r)$ is convergent, the rate of convergence is likely to be slow for the values of $x$ just listed.

The way in which Martin's approximate solution departs from the data for larger values of $(\alpha x/r)$ is of importance. Figure 1 contains a plot of Martin's solution for the azimuthal velocity distribution for the conditions given by Morton et al. The points have been determined from Fig. 4 of Ref. 1. Except for the zero spin case, the agreement between calculation and experiment is remarkably good. If the data in Fig. 3 are for the same conditions as Fig. 4 of Ref. 1, the measured longitudinal velocity profiles can be compared with the calculated profiles. Theoretically, the spin should have no

effect on the longitudinal velocity profile when $\alpha = 0$.† The difference between theory and experiment shown in Fig. 3 of Ref. 1 is small and may be due to a nose effect or some other experimental factor. In Fig. 2 the longitudinal velocity component profiles are compared at $\alpha = 3$ deg and for $\theta = 90$ deg and 270 deg. Here the differences are too large to be quantitatively acceptable.

Thus we conclude that the first place where the consequences of the large value of the expansion parameter $(\alpha x/r)$ appear is the longitudinal velocity component, and hence in the formula for the displacement thickness.

†If the flow is axially symmetric, that is, if the flow of an incompressible fluid is independent of azimuthal coordinate, the azimuthal momentum equation is uncoupled from the longitudinal momentum equation and the mass conservation equation.

Note that basic trends are not obscured even when $(\alpha x/r)$ is of the order of one-half.


## Acknowledgment

Research supported by the U.S. Army Research Office under Contract DAAG29-75-C-0001.


## References


[1]Morton, J.B., Jacobson, I.D., and Saunders, S., "Experimental Investigation of the Boundary Layer on a Rotating Cylinder," *AIAA Journal*, Vol. 14, Oct. 1976, pp. 1458-1463.

[2]Martin, J.C., "On Magnus Effects Caused by the Boundary Layer Displacement Thickness on Bodies of Revolution at Small Angles of Attack," Ballistic Research Laboratory Report 870 (Revised), Aberdeen Proving Ground, Md., 1955.


# Errata

## Model Predictions of Latitude-Dependent Ozone Depletion due to Supersonic Transport Operations


W.J. Borucki, R.C. Whitten, V.R. Watson,
and
H.T. Woodward
*NASA Ames Research Center, Moffett Field, Calif.*
C.A. Riegel and L.A. Capone
*Sand Jose State University, San Jose, Calif.*
and
T. Becker
*Informatics, Inc., Palo Alto, Calif.*


[AIAA J. **14**, 1738-1745 (1976)]

IN the process of paging, some of the text on page 1739 was transposed. The text of page 1739 should read as follows:

. . .except $HNO_3$, $NO_2$, $O_3$, $N_2O$, $HC\ell$, and $H_2O_2$ is chemical equilibrium. Because $HNO_3$, $HC\ell$, and $H_2O_2$ are water soluble, their number densities are set equal to zero at the lower boundary. The number densities of $NO_2$ and $N_2O$ are fixed at $3\times10^9$ cm$^{-3}$ and $7.5\times10^{12}$ cm$^{-3}$, respectively, at the lower boundary while that of $O_3$ is fixed at $6\times10^{11}$ cm$^{-3}$ (see Ref. 9).

The chemistry employed in this model is a simplified version of that used in our one-dimensional model studies.[10] At each time step, the model calculates the concentrations of $O_3$, $O(^3P)$, $O(^1D)$, $NO_2$, NO, $NO_3$, $N_2O$, $N_2O_5$, $HNO_3$, $HNO_2$, $H_2O_2$, $HO_2$, N, OH, H, $C\ell$, $C\ell O$, and $HC\ell$. The profiles of $N_2$, $O_2$, $H_2O$, $H_2$, $CH_4$, CO, and $CO_2$ are held fixed (at the experimentally determined values) during the calculations.

The rate coefficients are shown in Table 1, and the photolysis rates at zero optical depth are given in Table 2.

### Transport

The mean meridional circulation is obtained by the kinematic method from the averaged equation of mass continuity. With the assumption that the density field is in a steady state, the approximate form of this equation in spherical coordinates is

$$\frac{1}{R\cos\phi}\frac{\partial(\bar{\rho}\bar{v}\cos\phi)}{\partial\phi}+\frac{\partial(\bar{\rho}\bar{w})}{\partial z}=0 \qquad (5)$$

where the overbar denotes an average with respect to time and longitude, $\bar{\rho}$ is the bulk density, $\bar{v}$ and $\bar{w}$ are the meridional and vertical velocity components, $R$ is the radius of the earth, and $\phi$ the latitude. Equation (5) implies the existence of a "stream function" $\psi$ for the total mass flux such that

$$2\pi R\bar{\rho}\bar{v}\cos\phi=-\frac{\partial\psi}{\partial z} \qquad 2\pi R\bar{\rho}\bar{w}\cos\phi=\frac{\partial\psi}{R\partial\phi} \qquad (6)$$

If the distrubution of $\bar{\rho}$ and $\bar{v}$ is known, the first of these can be integrated vertically, and $\bar{w}$ can be obtained from the second.

Up to 20 km, the density was obtained from data presented by Oort and Rasmusson,[46] and above that altitude by vertical integration of the hydrostatic equation, using mean (rocket) temperatures.[47]

The $\bar{v}$ components were based on the results[46] up to 20 km. These values were then extrapolated to the top of the model by imposition of a simple vertical profile that matched the 20-km value and satisfied the kinematic constraint that there be no. . .

Received Feb. 18, 1977.
Index category: Atmospheric, Space, and Oceanographic Sciences.